Electronic Supplementary Material (ESI) for ChemComm.

Supporting Information

for

A spin-canted Ni^{II}_4-based metal-organic framework with gas sorption properties and high adsorptive selectivity for light hydrocarbons

Jia Li,[a] Ying Guo,[a] Hong-Ru Fu,[b] Jian Zhang,[b] Rong-Bin Huang,[a] Lan-Sun Zheng[a] and Jun Tao*[a,c]

[a]*State Key Laboratory of Physical Chemistry of Solid Surfaces & Department of Chemistry, College of Chemistry and Chemical Engineering, Xiamen University, Xiamen 361005, People's Republic of China. Tel: 0086-592-2188138; Fax: 0086-592-2183047. E-mail: taojun@xmu.edu.cn*

[b]*Fujian Institute of Research on the Structure of Matter, Chinese Academy of Science, Fuzhou 350002, People's Republic of China.*

[c]*Collaborative Innnovation Center of Chemistry for Energy Materials, Xiamen University, Xiamen 361005, People's Republic of China.*

Contents

I) Experimental Section

Materials and Methods. Chemicals were purchased from commercial sources and were used without further purification. Thermogravimetric analysis was performed on a NETZSCH TG 209 thermobalance in nitrogen atmosphere, sample was placed in alumina container and data were recorded at 10 °C/min between 20 and 1000 °C. IR spectra (KBr pellet) were obtained from a Nicolet 5DX spectrometer in the region of 400–4000 cm^{-1}. Powder X-ray diffraction data (PXRD) was collected on a Bruker D8 ADVANCE diffractometer at room temperature using Cu $K\alpha$ (λ = 1.5418 Å) radiation. Elemental analysis of carbon, hydrogen and nitrogen was carried out on a Vario EL III analyzer. The single-crystal X-ray diffraction data of **1**·*S* were collected on an Agilent Technologies SuperNova X-ray diffractometer with Mo $K\alpha$ radiation (λ = 0.71073 Å) at 100 K. The data were processed using CrysAlisPro.[1] The structure was solved and refined using Full-matrix least-squares based on F^2 with program SHELXS-97 and SHELXL-97[2] within Olex2.[3] Gas sorption isotherms were performed on Micromeritics ASAP 2020 and Trist 3020 apparatuses. Magnetic susceptibility measurements were carried out on a Quantum Design MPMS XL7 SQUID magnetometer. Magnetic data were calibrated with the sample holder, and diamagnetic corrections were estimated from Pascal's constants.

1. CrysAlisPro Version 1.171.35.19, (2011). Agilent Technologies Inc. Santa Clara, CA, USA.
2. G. M. Sheldrick, A short history of SHELX, *Acta Cryst.*, 2008, **A64**, 112-122.
3. Dolomanov et al. OLEX2: a complete structure solution, refinement and analysis program, *J. Appl. Cryst.*, 2009, **42**, 339-341.

Synthesis of $[Ni_4(OH)_2(ina)_2(dpda)_2(H_2O)_3]\cdot(H_2O)_9(C_2H_6O)_3$ (1·*S*): Solid $Ni(NO_3)_2\cdot 6H_2O$ (0.147 g, 0.5 mmol) was added without stirring to an EtOH/H_2O (10 mL, v/v = 5:5) solution containing isonicotinic acid (0.025 g, 0.2 mmol), 2,6-dimethyl-pyridine-3,5-dicarboxylic acid (dpdaH_2, 0.0976 g, 0.5 mmol) and NaOH (0.045 g, 1.1 mmol). The mixture was sealed in a 23 mL Teflon-lined stainless steel vessel and heated to 170 °C within 500 min, maintained at this temperature for 3600 min and then cooled to 30 °C within 2880 min. Green block crystals of **1**·*S* were obtained by filtration. Yield: ~62% based on $Ni(NO_3)_2\cdot 6H_2O$. Elemental analysis calcd (%) for $C_{36}H_{66}N_4Ni_4O_{29}$: C 34.49, H 5.31, N 4.47. Found: C 34.35, H 5.35, N 4.43. IR (KBr, cm^{-1}): 3408, 1611, 1429, 1382, 1160, 1058, 1027, 792, 777, 691.

II) Tables

Table 1. Crystal data and structure refinements for compound **1**·*S*.

	1·*S*
formula	$Ni_4C_{30}H_{30}O_{17}N_4$
M_r / g mol^{-1}	953.35
cryst syst	monoclinic
space group	$P2_1/c$
a / Å	12.8539(5)
b / Å	14.4578(8)
c / Å	30.4530(17)
α / deg	90
β / deg	96.497(5)
γ / deg	90
V / Å^3	5623.05
Z	4
D_c / g cm^{-3}	1.124
μ / mm^{-1}	1.371
reflns collected	28515
GOF	0.966
R_{int}	0.0464
R1 ($I > 2\sigma(I)$) [a]	0.0664
wR2 (all data)	0.1204

[a] $R1 = ||F_o| - |F_c||/|F_o|$; $wR2 = \{[w(F_o^2 - F_c^2)^2]/[w(F_o^2)^2]\}^{1/2}$; $w = 1/[\sigma_2(F_o^2) + (ap)^2 + bp]$, where $p = [\max(F_o^2, 0) + 2F_c^2]/3$; and $Rw = [w(|F_o| - |F_c|)^2/w|F_o|^2]^{1/2}$, where $w = 1/\sigma^2(|F_o|)$.

Table S2. Selected bond lengths (Å) and angles (deg) in **1**·*S*.

1·*S*			
Ni(1)-O(13)	2.008(2)	Ni(3)-O(13)	2.038(2)
Ni(1)-O(2)	2.030(2)	Ni(3)-O(6)	2.044(2)
Ni(1)-O(7a)	2.042(2)	Ni(3)-O(10)	2.056(2)
Ni(1)-O(11b)	2.075(2)	Ni(3)-O(14)	2.060(2)
Ni(1)-O(3W)	2.094(3)	Ni(3)-N(4)	2.071(3)
Ni(1)-O(4c)	2.149(2)	Ni(3)-O(1)	2.096(2)
Ni(2)-O(14)	2.003(2)	Ni(4)-O(14)	2.032(2)
Ni(2)-O(3c)	2.045(2)	Ni(4)-O(8a)	2.047(2)
Ni(2)-O(5)	2.049(2)	Ni(4)-O(13)	2.049(2)
Ni(2)-O(2W)	2.066(3)	Ni(4)-O(9)	2.051(2)
Ni(2)-O(1W)	2.065(3)	Ni(4)-N(3d)	2.062(3)
Ni(2)-O(1)	2.162(2)	Ni(4)-O(4c)	2.100(2)
Ni(3)-Ni(4)	2.9127(6)		
Ni(3)-O(1)-Ni(2)	91.30(9)	Ni(3)-O(13)-Ni(4)	90.89(9)
Ni(4c)-O(4)-Ni(1c)	91.78(9)	Ni(2)-O(14)-Ni(4)	130.64(12)
Ni(1)-O(13)-Ni(3)	130.11(12)	Ni(2)-O(14)-Ni(3)	97.07(10)
Ni(1)-O(13)-Ni(4)	97.52(10)	Ni(4)-O(14)-Ni(3)	90.75(9)

Symmetry codes: (a) *x* – 1, *y*, *z*; (b) – *x* + 2, – *y* + 1, – *z*; (c) – *x* + 2, – *y* + 2, – *z*; (d) – *x* + 2, *y* + 1/2, – *z* + 1/2; (e) *x* + 1, *y*, *z*; (f) – *x* + 2, *y* – 1/2, – *z* + 1/2.

Table S3. Virial graph analysis data for the activated **1**, and the separation selectivity of C2 hydrocarbons over methane.

	T	K_H	A_0	A_1	R^2	$S_{i/j}$[a]	Q_{st}
	(K)	(mol g^{-1} Pa^{-1})	ln(mol g^{-1} Pa^{-1})	(g mol^{-1})			(kJ mol^{-1})
CH_4	273	1.351×10^{-8}	–18.120±0.002	–315.971±9.778	0.99428		12.1
	297	8.8×10^{-9}	–18.549±0.002	–301.214±6.867	0.99534		
C_2H_2	273	8.299×10^{-7}	–14.002±0.006	–663.390±20.783	0.99609	61.5	31.8
	297	2.540×10^{-7}	–15.186±0.003	–411.872±13.049	0.99401	28.9	
C_2H_4	273	3.651×10^{-7}	–14.823±0.002	–338.414±6.860	0.99713	27.0	26.7
	297	1.419×10^{-7}	–15.768±0.002	–238.645±0.002	0.99301	16.1	
C_2H_6	273	6.032×10^{-7}	–14.321±0.002	-338.686±5.653	0.99861	44.7	23.5
	297	2.515×10^{-7}	-15.196±0.002	-201.931±9.035	0.99204	28.6	

[a] The Henry's Law selectivity for gas component *i* over *j* is calculated based on: $S_{i/j} = K_H(i) / K_H(CH_4)$.

Table S4. 3D MOFs with Co^{II} or Ni^{II} clusters showing the coexistence of spin canting and spin-glass behaviors.

Compounds	Clusters	Nets
$[Co_8(OH)_4(SO_4)_2(L1)_4(H_2O)_4]\cdot$solvents[12b]	Co_8	(3,12)-connected
$[Co_7(OH)_4(H_2O)_2(L2)_4(L3)_3]\cdot$solvents[12a]	Co_7	8-connected
$[Ni_7(OH)_4(H2O)_2(L2)_4(L3)_3]\cdot$solvents[12a]	Ni_7	8-connected
$[Co_4(L2)_5(OH)_2(H_2O)(EtOH)]\cdot NO_3\cdot$solvents[12c]	Co_4	7-connected
$[Ni_4(L2)_5(OH)_2(EtCOO)]\cdot$solvents[12c]	Ni_4	9-connected
1[this work]	Ni_4	6-connected

L1 = 2,6-dicarboxyphenyl-4,4′-bipyridine; L2 = isonicotinate; L3 = isophthalate.

III) Additional Figures

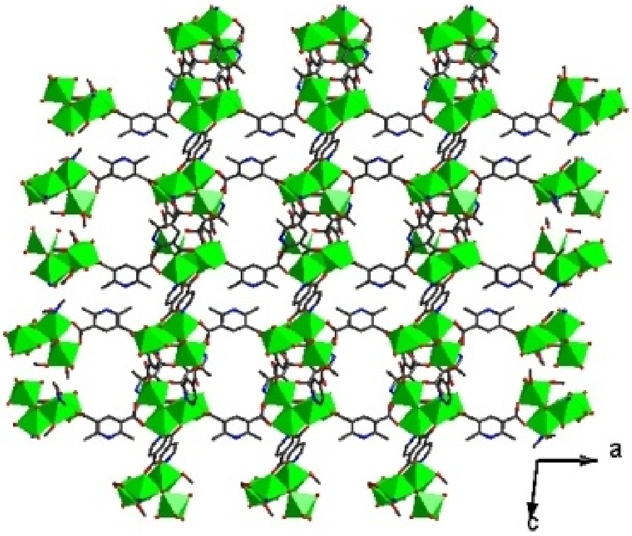

Fig. S1 The three-dimensional structure of **1** viewed along the *b* axis.

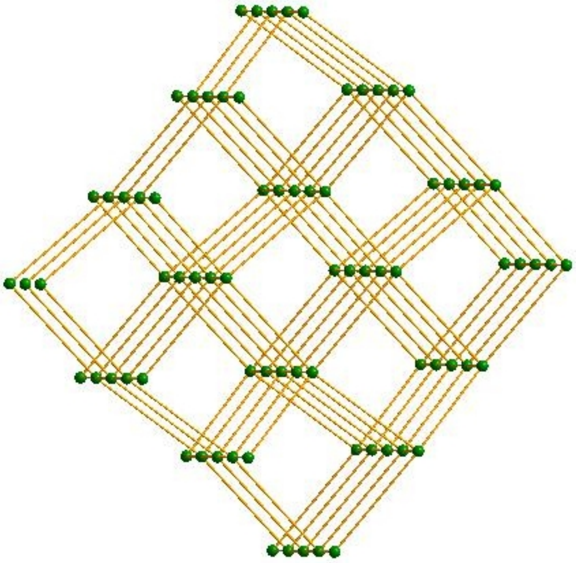

Fig. S2 The uninodal 6-connected topological structure of **1**.

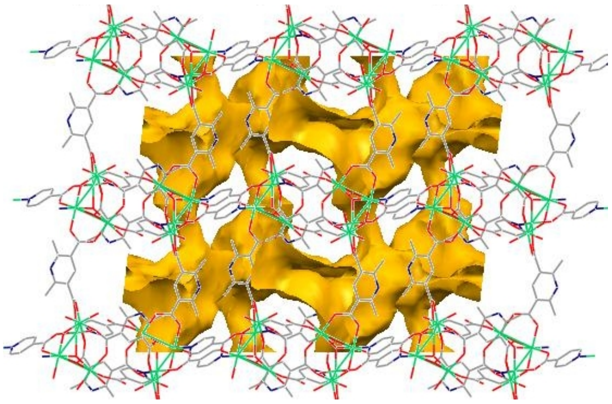

Fig. S3 Accessible surfaces of **1**.

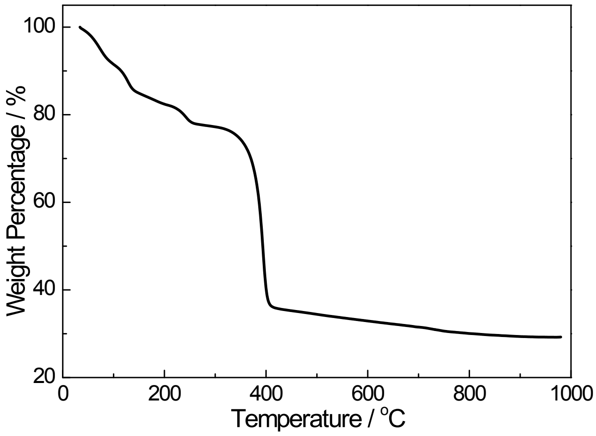

Fig. S4 TGA of **1**·*S*.

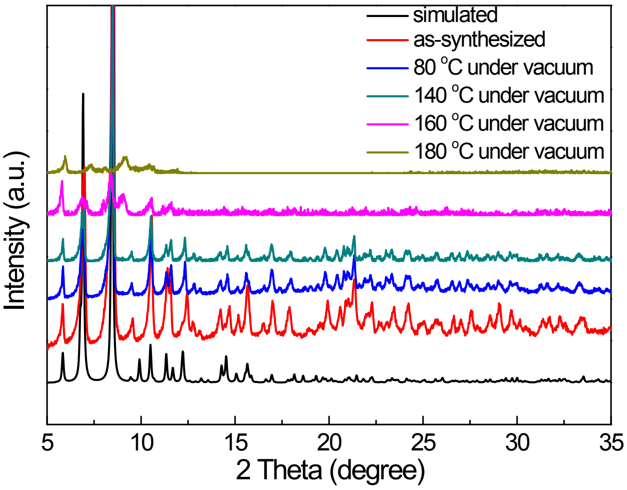

Fig. S5 Powder X-ray diffraction pattern of the desolvated framework **1** obtained under various temperature and high vacuum.

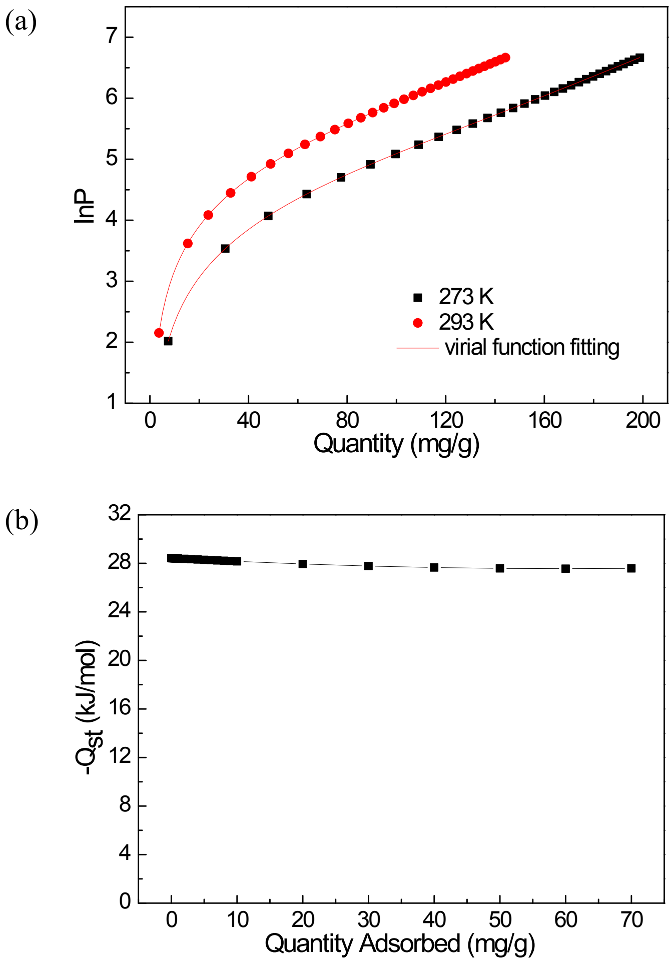

Fig. S6 Virial fitting (lines) of the CO_2 adsorption isotherms (points) measured at 273 and 293 K (a), respectively, and the enthalpy of CO_2 adsorption (b).

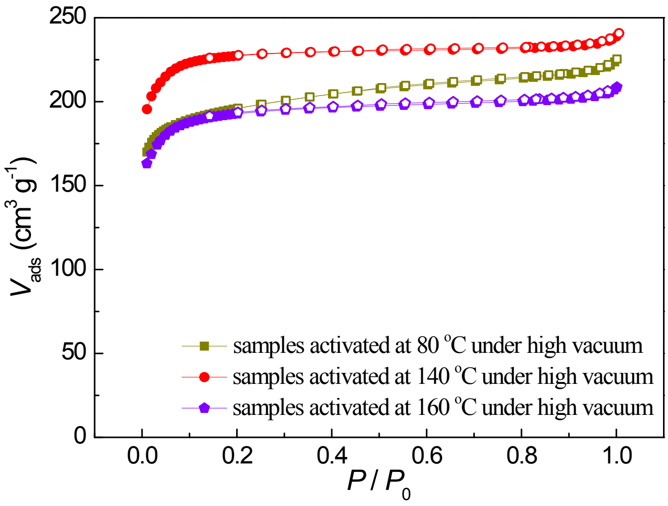

Fig. S7 Nitrogen adsorption isotherms of **1** activated at different temperatures.

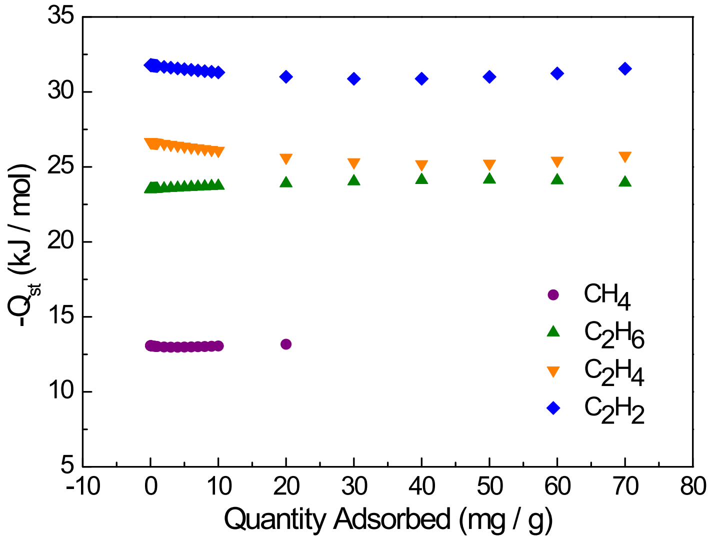

Fig. S8 The adsorption heats for C_2H_2, C_2H_4, C_2H_6 and CH_4.

(a)

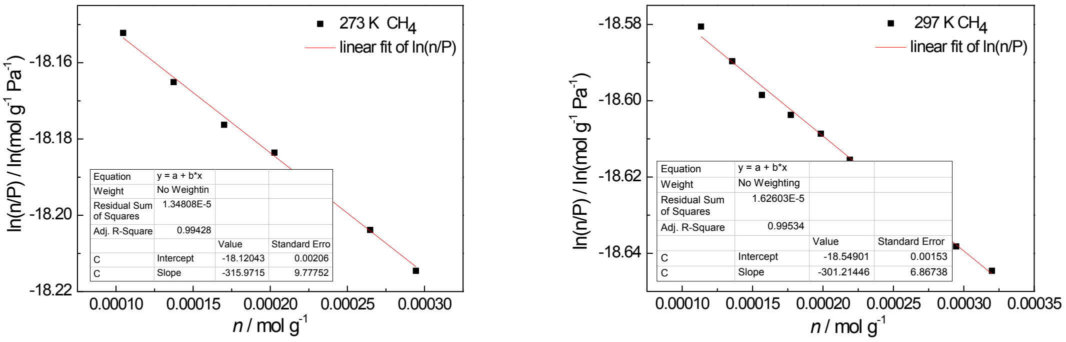

Equation	y = a + b*x		
Weight	No Weightin		
Residual Sum of Squares	1.34808E-5		
Adj. R-Square	0.99428		
		Value	Standard Erro
C	Intercept	-18.12043	0.00206
C	Slope	-315.9715	9.77752

Equation	y = a + b*x		
Weight	No Weighting		
Residual Sum of Squares	1.62603E-5		
Adj. R-Square	0.99534		
		Value	Standard Error
C	Intercept	-18.54901	0.00153
C	Slope	-301.21446	6.86738

(b)

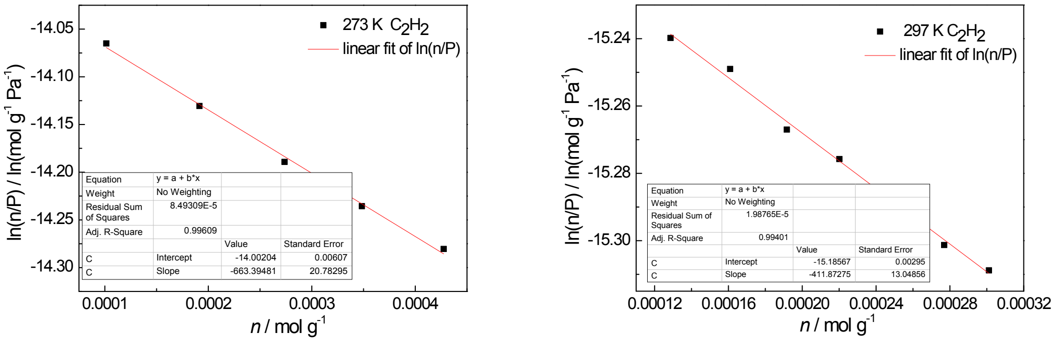

Equation	y = a + b*x		
Weight	No Weighting		
Residual Sum of Squares	8.49309E-5		
Adj. R-Square	0.99609		
		Value	Standard Error
C	Intercept	-14.00204	0.00607
C	Slope	-663.39481	20.78295

Equation	y = a + b*x		
Weight	No Weighting		
Residual Sum of Squares	1.98765E-5		
Adj. R-Square	0.99401		
		Value	Standard Error
C	Intercept	-15.18567	0.00295
C	Slope	-411.87275	13.04856

(c)

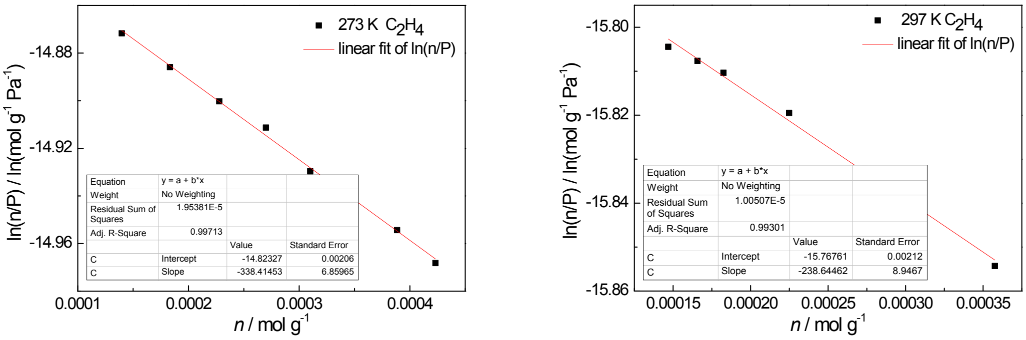

Equation	y = a + b*x		
Weight	No Weighting		
Residual Sum of Squares	1.95381E-5		
Adj. R-Square	0.99713		
		Value	Standard Error
C	Intercept	-14.82327	0.00206
C	Slope	-338.41453	6.85965

Equation	y = a + b*x		
Weight	No Weighting		
Residual Sum of Squares	1.00507E-5		
Adj. R-Square	0.99301		
		Value	Standard Error
C	Intercept	-15.76761	0.00212
C	Slope	-238.64462	8.9467

(d)

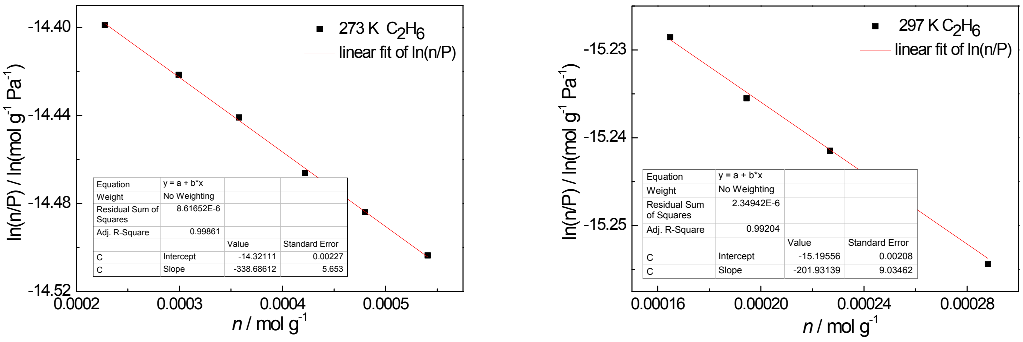

Equation	y = a + b*x		
Weight	No Weighting		
Residual Sum of Squares	8.61652E-6		
Adj. R-Square	0.99861		
		Value	Standard Error
C	Intercept	-14.32111	0.00227
C	Slope	-338.68612	5.653

Equation	y = a + b*x		
Weight	No Weighting		
Residual Sum of Squares	2.34942E-6		
Adj. R-Square	0.99204		
		Value	Standard Error
C	Intercept	-15.19556	0.00208
C	Slope	-201.93139	9.03462

Fig. S9 The virial graphs for adsorption of CH_4 (a), C_2H_2 (b), C_2H_4 (c) and C_2H_6 (d) in **1** at 273 K (Left) and 297 K (Right).

(a)

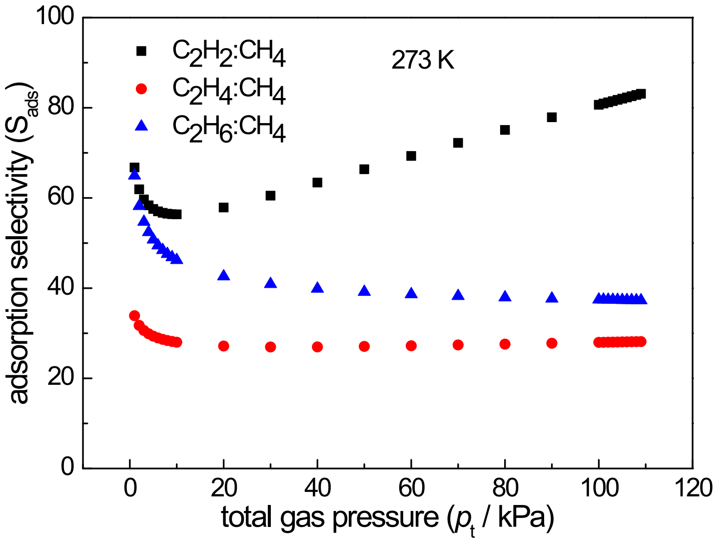

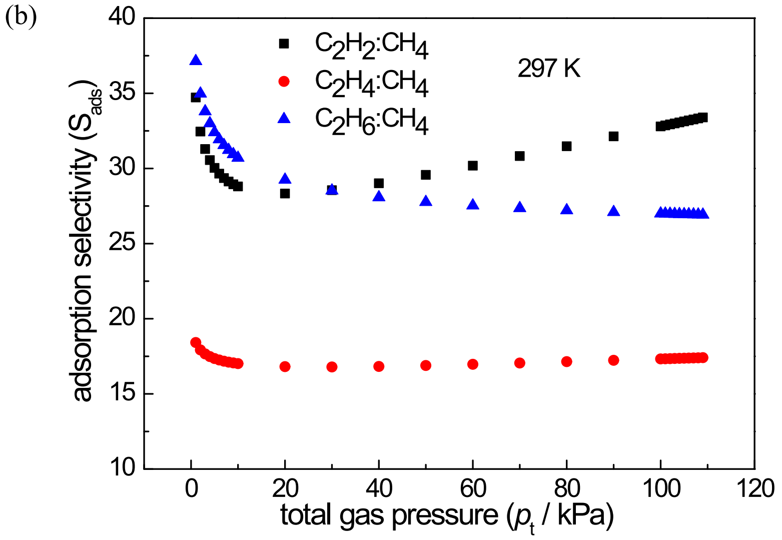

Fig. S10 IAST calculations of the C_2H_6/CH_4、C_2H_4/CH_4 and C_2H_2/CH_4 adsorption selectivity of **1** for adsorption from an equimolar mixture at total bulk gas phase at 273K (a) and 297 K (b).

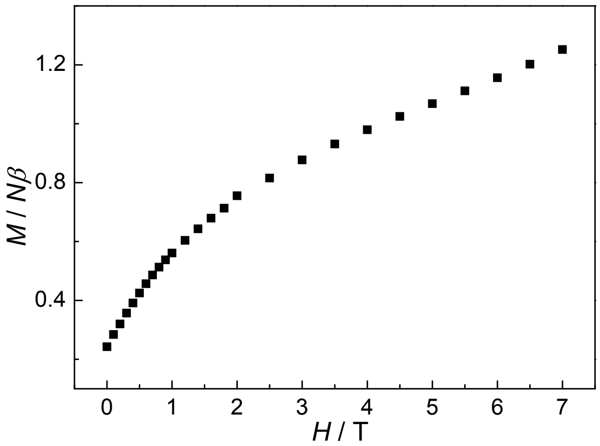

Fig. S11 Field-dependent magnetization of **1**·S at 2 K.

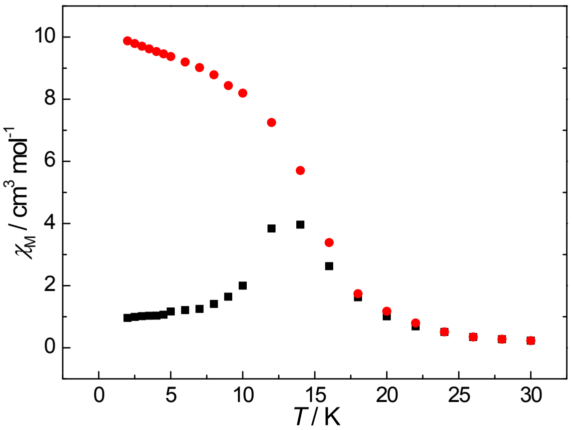

Fig. S12 ZFC-FC magnetization versus temperature of **1**·*S*.

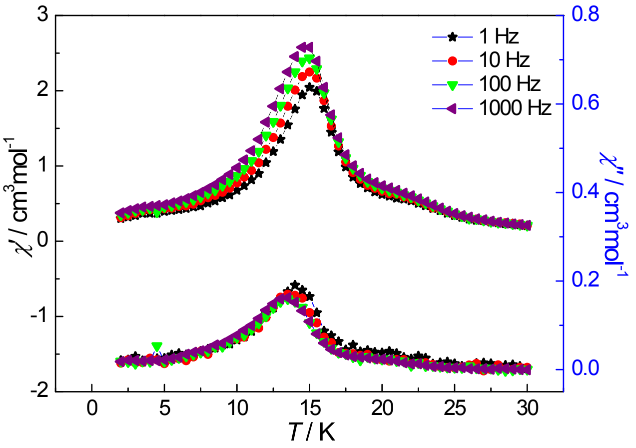

Fig. S13 ac magnetic susceptibility of **1**·*S*.

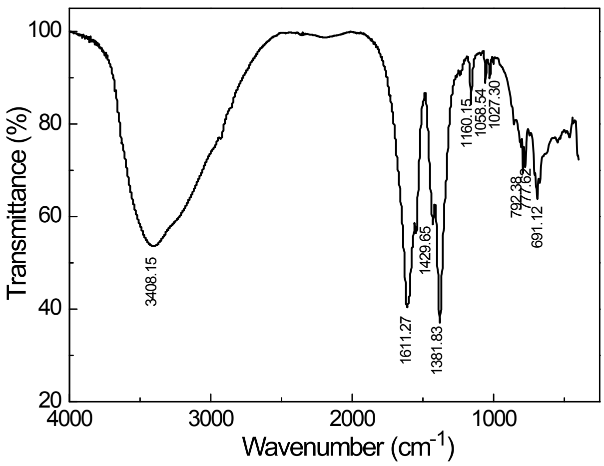

Fig. S14 Infrared spectra of **1**·*S*.